Retinal Neurovascular Impairment in Full-Course Diabetic Retinopathy: The Guangdong Diabetic Retinopathy Multiple-Omics Study

Chunran Lai,[1,2] Ting Su,[2] Jiahui Cao,[2] Qinyi Li,[1,2] Zijing Du,[2] Yaxin Wang,[2] Shan Wang,[2] Qiaowei Wu,[2] Yijun Hu,[2] Ying Fang,[2] Huiyi Liao,[2] Zhuoting Zhu,[3] Xianwen Shang,[4] Mingguang He,[2,4] Honghua Yu,[1,2,5] and Xiayin Zhang[2]

[1]School of Medicine, South China University of Technology, Guangzhou, China
[2]Guangdong Eye Institute, Department of Ophthalmology, Guangdong Provincial People's Hospital (Guangdong Academy of Medical Sciences), Southern Medical University, Guangzhou, China
[3]Centre for Eye Research Australia, Royal Victorian Eye and Ear Hospital, Melbourne, Australia
[4]School of Optometry, The Hong Kong Polytechnic University, Hong Kong, China
[5]Guangdong Provincial Key Laboratory of Artificial Intelligence in Medical Image Analysis and Application, Guangzhou, China

Correspondence: Mingguang He, Guangdong Provincial People's Hospital, Guangdong Academy of Medical Sciences, No. 106, Zhongshan Second Road, Yuexiu District, Guangzhou 510080, China; hemingguang@gdph.org.cn.
Honghua Yu, Guangdong Provincial People's Hospital, Guangdong Academy of Medical Sciences, No. 106, Zhongshan Second Road, Yuexiu District, Guangzhou 510080, China; yuhonghua@gdph.org.cn.
Xiayin Zhang, Guangdong Provincial People's Hospital, Guangdong Academy of Medical Sciences, No. 106, Zhongshan Second Road, Yuexiu District, Guangzhou 510080, China; zhangxiayin@gdph.org.cn.

CL and TS contributed equally to the study and are to be considered joint first authors.

Received: June 16, 2024
Accepted: November 7, 2024
Published: December 10, 2024

Citation: Lai C, Su T, Cao J, et al. Retinal neurovascular impairment in full-course diabetic retinopathy: The guangdong diabetic retinopathy multiple-omics study. *Invest Ophthalmol Vis Sci.* 2024;65(14):20. https://doi.org/10.1167/iovs.65.14.20

Purpose. The purpose of this study was to explore the succession of the central and peripheral neurovascular and microstructural impairments in patients with full-course diabetic retinopathy (DR), consisting of preclinical DR, nonproliferative DR (NPDR), and proliferative DR (PDR).

Methods. Our analysis included 81 participants (including 23 healthy controls, 23 with preclinical DR [diabetes without retinopathy], 13 with NPDR, and 22 with PDR) from the Guangdong Diabetic Retinopathy Multiple Omics Study. Retinal structure and function were evaluated and quantified using ultra-widefield swept-source optical coherence tomography angiography (UWF-SS-OCTA), electroretinography (ERG), and adaptive optics scanning laser ophthalmoscopy (AOSLO). Correlation analysis was conducted to explore the relationship between structural parameters and functional parameters.

Results. In the preclinical DR group, decreased amplitude in the DR assessment protocol were observed ($P = 0.003$), with no changes in structure and photoreceptor cells (all $P > 0.05$). In the NPDR group, photoreceptor cells were impaired (all $P < 0.05$) with delayed implicit time in the International Society for Clinical Electrophysiology of Vision (ISCEV) Photopic flicker protocol, increased macular and inner nuclear layer thickness, and decreased vessel density and perfusion area of the deep capillary plexus (all $P < 0.05$). In the PDR group, delayed implicit time and decreased amplitude in the ISCEV Photopic flicker and photopic negative response (PhNR) protocol, and neurovascular impairments were observed (all $P < 0.05$). Correlation analysis demonstrated a significant correlation between functional parameters and various structural indicators (all $P < 0.05$).

Conclusions. The cone pathway function began to decline in preclinical DR and distinct photoreceptor cell disorders were observed in NPDR. Notably, instruments with a wider field of view or more detailed microscopic techniques will provide enhanced neurovascular imaging, offering fresh insights into full-course DR.

Keywords: full-course diabetic retinopathy (full-course DR), diabetic retinopathy (DR), neurovascular damage, adaptive optics

Diabetic retinopathy (DR) is conventionally categorized as a microvascular complication of DM, standing as a prominent cause of global blindness.[1] It is also known as a neurovascular disorder characterized by the disruption of the retinal neurovascular unit (NVU), composed of retinal neurons, glia, and vascular cells.[2] Identification of NVU changes may lead to more effective prevention and treatment strategies for DR.[2] However, studies addressing NVU changes in DR focus solely on individual phases of the disease, lacking a comprehensive understanding of DR as a whole,[3,4] and understanding the full course of the disease is conducive to its prevention and intervention.[5,6] Thus, it becomes imperative to identify and monitor NVU alterations in the full-course DR.

Studies indicated that NVU changes impact the structure and function of the retina in patients with DR.[4,7–10] Diminutions in the thickness of the ganglion cell complex layer and retinal nerve fiber layer, and capillary vessel density (VD) were observed in the preclinical DR group.[4,7,9] Compared with the preclinical DR group, the nonproliferative DR (NPDR) group's central subfoveal thickness was higher.[3] In the proliferative DR (PDR) group, decreased retinal VD at the superficial capillary plexus (SCP) and deep capillary plexus (DCP) were found.[10] As for retinal function, delayed implicit time and decreased amplitude found in electroretinographic studies occur in individual phases of DR.[8,11] Although studies have demonstrated changes in the structure and function of the NVU at different stages of DR, the topic remains to be explored in depth. There is still a lack of a comprehensive understanding of the full course of DR. It is necessary to clarify NVU alterations in full-course DR using electrophysiology and ophthalmic instruments with new technology, such as ultra-widefield swept-source optical coherence tomography angiography (UWF-SS-OCTA) and adaptive optics scanning laser ophthalmoscopy (AOSLO).

The UWF-SS-OCTA has an ultra-wide field of view that allows visualization of peripheral retinal damage.[12] AOSLO enables evaluation of the living human retinal vasculature at the cellular level, offering insight into the microstructural impairments.[13] It has been applied to identify vascular biomarkers in DR and detected that decreased regularity of the cone arrangement is consistently associated with increasing DR severity.[14,15]

In this study, we aimed to present the combined NVU results in full-course DR by using the UWF-SS-OCTA, AOSLO, and electroretinography (ERG). We analyzed the thickness, blood perfusion, and functional changes throughout the full-course DR in the central and peripheral retina. We assessed photoreceptor damage in the progression of DR. Furthermore, we evaluated the associations between structural and functional impairments across the DR process.

Methods

Study Population

The GD-RMOS study is a hospital-based cohort study recruiting 114 participants aged 35 to 85 years from January 2023 to March 2024 in Guangzhou, China. Written informed consent was obtained from all participants. Participants in the cohort study have provided various blood and intraocular fluids for multi-omics analysis, which includes the examination of the transcriptome, proteome, metabolome, and other omics data. Concurrently, they have undergone a series of ophthalmic examinations, such as ERG, UWF-SS-OCTA, and AOSLO, etc. This study was approved by the Medical Research Ethics Committee of the Guangdong Provincial People's Hospital (KY2023-1210-02) and adhered to the tenets of the Declaration of Helsinki.

Ascertainment of T2DM and Full-Course DR

The diagnosis of type 2 diabetes mellitus (T2DM) was established by endocrinologists according to the diagnostic criteria of the American Diabetes Association.[16] The concept of the full-course DR emphasized in this study includes three stages of the DR: preclinical DR (refers to patients with diabetes without clinically detectable retinopathy), NPDR, and PDR. The diagnosis and classification of DR were confirmed according to the international clinical diabetic retinopathy based on color fundus images.[17] If both eyes were eligible, one eye was randomly selected for the study. Exclusion criteria included: (1) other ocular conditions (glaucoma, uveitis, retinal vein, or artery occlusion); (2) history of ocular surgery; (3) intraocular pressure > 21 millimeters of mercury (mm Hg); and (4) the inability to cooperate with the eye examination.

Full-Field Flicker Electroretinography

The RETeval system (LKC Technologies, Inc., Gaithersburg, MD, USA) is a small, handheld, mydriasis-free full-field flicker ERG recording device that provides constant retinal illuminance across different pupil sizes using the equation: photopic flash retinal illuminance (Td·s) = photopic flash luminance (cd-s/m^2) × pupillary area (mm^2). Thus, pupil dilation is unnecessary for consistent results. The device was used according to the manufacturer's instructions, as described in previous studies.[18,19] Three different protocols were selected. First, the "DR assessment protocol" in the current study was chosen to assess the cone pathway in the inner retina. The protocol defaults the flash retinal illuminance as 16 and 32 photopic Td·s. A 28.3 hertz (Hz) flickering white-light stimulus was produced by brief flashes (<1 ms) in the ganzfeld. Second, the International Society for Clinical Electrophysiology of Vision (ISCEV) Photopic Flicker, Td protocol was used to overview the functionality of the bipolar cell pathways.[20] The ISCEV Photopic Flicker defaults the flash retinal illuminance as 85 photopic Td·s with a 28.3 Hz flickering white-light stimulus. Third, the photopic negative response (PhNR) 3.4 Hz Td Long protocol was used to overview the functionality of the retinal ganglion cells.[21] The PhNR protocol has a red flash (1.0 cd·s/m^2 or 38 Td·s) on a blue background (10 cd/m^2 or 380 Td), with 3.4 Hz stimulus frequency and 200 (long protocol) flashes. A special sensor strip skin electrode can monitor the electrical activity of the retina and parameters, including that the implicit time and amplitudes were obtained in three protocols.

Ultra-Widefield Swept-Source Optical Coherence Tomography Angiography

After pupil dilation, macular imaging was performed using UWF-SS-OCTA (VG200D; SVision Imaging, Ltd., China), as previously described.[12] The scanning mode "Angio 26 × 21 1280 × 1034 R2" was chosen in this study with a 130-degree inner eye angle, centered on the fovea. Each scan comprised 1280 A-scans with 1034 A-scans per B-scan, repeated twice, and the average value was used to improve the signal-to-noise ratio (SNR). The instrument was equipped with an eye-tracking utility and had a combining follow-up mode to eliminate eye-motion artifacts. Images with signal intensity ≥6 were included in the data analysis. The UWF-SS-OCTA images were automatically segmented using the built-in van Gogh version 1.36.10 instrument software and exported for further analysis. The software automatically fits a circle (1.0 mm in diameter) centered on the fovea. The perifovea region is defined as a 21.0 mm wide round annulus around the fovea 1.0 mm circle and the perifovea is defined as a 26.0 mm wide round annulus around the parafovea. The following parameters were quantified: the thickness of the ganglion cell layer (GCL) and internal plexiform layer (IPL), inner nuclear layer (INL), and retina; the VD and perfusion

Investigative Ophthalmology & Visual Science

area (PA) of superficial vascular plexus (SVP), intermediate capillary plexus (ICP), and DCP.

Adaptive Optics Scanning Light Ophthalmoscopy

After pupil dilation, a subgroup was divided to undergo AOSLO imaging with a commercialized AOSLO system (Mona IIa, Robotrak Technologies, Nanjing, China) to obtain high-resolution and visual enface images of the retinal cells.[22] This system utilizes an 840 nm light source with a full-width half-maximum of 40 nm. The field of view on the retina spans 2.4 × 2.4 degrees (approximately 700 × 700 µm). The AOSLO system is equipped with a real-time retina tracking module, ensuring eye-motion stabilization and efficient imaging. To capture high-quality images, each retinal location is imaged for approximately 3 seconds, resulting in approximately 40 frames. These frames undergo a de-warping process to eliminate distortion introduced by the sinusoidal motion of the resonant scanner. Subsequently, an automatic detection system identifies and removes invalid frames caused by blinking or saccades, ensuring only the most reliable frames are retained. Finally, a strip-based registration process is used. The aligned frames are averaged to improve the SNR. The entire process takes place right after each imaging session and will automatically generate a registered image by the Mona IIa software. For quantitative cell analysis, the software uses an artificial intelligence (AI)-based algorithm for automatic photoreceptor segmentation and generates statistical descriptors of photoreceptor morphology properties like cone density, nearest neighbor distance (NND), dispersion, and regularity.[22]

Covariates

All the participants underwent comprehensive ocular examinations, including best-corrected visual acuity, intraocular pressure, refractive error (auto-refractometry), and mydriatic slit-lamp fundus examination. Data on sex, age, smoking status, drinking status, and duration of T2DM of each patient were recorded, along with levels of glycated hemoglobin (HbA1c), estimated glomerular filtration rate (eGFR), and cholesterol. HbA1c was measured using ion-exchange liquid chromatography (Tosoh, Tokyo, Japan), and cholesterol was measured using the enzymatic colorimetric assay (Roche). The eGFR was calculated using the Chronic Kidney Disease Epidemiology Collaboration formula combining creatinine-cystatin C.[23]

Statistical Analysis

The 2-tailed test was used, the effect size was 0.341 according to Zeng Y's research,[8] α was 0.05, test efficacy (1-β) was 0.8, and the total sample size was 49. At present, the total sample size of this study is 81, which meets the conditions. The *t*-test was used to estimate the sample size before the correlation analysis. Baseline characteristics at different stages in full-course DR were compared using the *t*-test for continuous variables, and the chi-squared test for categorical variables. One-way analysis of variance (ANOVA) was used to assess differences in baseline characteristics, functional, and structural parameters across different stages of full-course DR. Spearman correlation analysis was conducted to evaluate the rank correlation between functional and structural parameters, adjusted for participant characteristics that were either significantly different at baseline in the different stages of full-course DR or previously associated with DR in people with diabetes. Covariates included age, diabetes duration, and HbA1c.

Reported *P* values are 2-sided and the results were considered statistically significant with a P value < 0.05. All analyses were performed using G·Power (version 3.1; University of Dusseldorf, USA), Stata (version 17; Stata Corp), and R (version 3.4.1; R Project for Statistical Computing, Vienna, Austria).

Results

Figure 1 shows the flow chart of our study design. The changes in retinal structure and function throughout the full course of DR are shown in Figure S1. After excluding individuals with missing data on ophthalmic examinations, 81 participants were enrolled in the study, including 23 healthy controls, 23 with preclinical DR, 13 with NPDR, and 22 with PDR. Table 1 shows the demographic and clinical data of the preclinical DR, NPDR, and PDR, and the healthy participants' group. At baseline, participants comprised 49.38% women, with a mean age (standard deviation [SD]) of 67.69 (SD = 9.74) years. Differences in baseline characteristics among the four groups are described in Table 1. Participants with DR were more likely to be older, with longer diabetes duration and higher HbA1c. However, gender, smoking status, drinking status, the condition of hypertension, eGFR, and cholesterol were comparable across the four groups (all $P > 0.05$). Twenty-six participants were divided into subgroups with a mean age (SD) of 68.25 (SD = 7.16) years, 57.69% women, including 6 healthy patients, 9 with preclinical DR, 6 with NPDR, and 5 with PDR (Supplementary Table S1).

The Transformation of ERG Parameters in Full-Course DR

The comparisons of the DR assessment protocol results among the different stages of full-course DR are demonstrated in Table 2. Compared with the control groups, the decreased amplitude of the cone pathway was first observed in the preclinical DR group in comparison to the control group (all $P < 0.05$). Then, delayed implicit time and decreased amplitude were found in the NPDR and PDR groups compared with the control groups (all $P < 0.05$). These results suggest that the cone pathway function begins to decline in preclinical DR and worsens with the progression of the disease. The implicit time of ISCEV Photopic flicker was delayed in NPDR ($P = 0.020$) and PDR ($P < 0.001$), with decreased amplitude observed in PDR ($P = 0.018$), which indicates the impairment of bipolar cell function begins from the NPDR stage (Supplementary Table S2). The delayed implicit time of PhNR was found in the PDR in comparison to the healthy controls ($P = 0.041$), representing impaired function of retinal ganglion cells (see Supplementary Table S2).

The Transformation of UWF-SS-OCTA Parameters During the Full-Course DR

Compared with the control group, the results for neural structures including the thickness of the macula, GCL + IPL, and INL were variable, whereas VD and PA of SVP, ICP, and DCP showed a decreasing trend at different stages of DR (Table 3). The thickness of the macula and INL increased

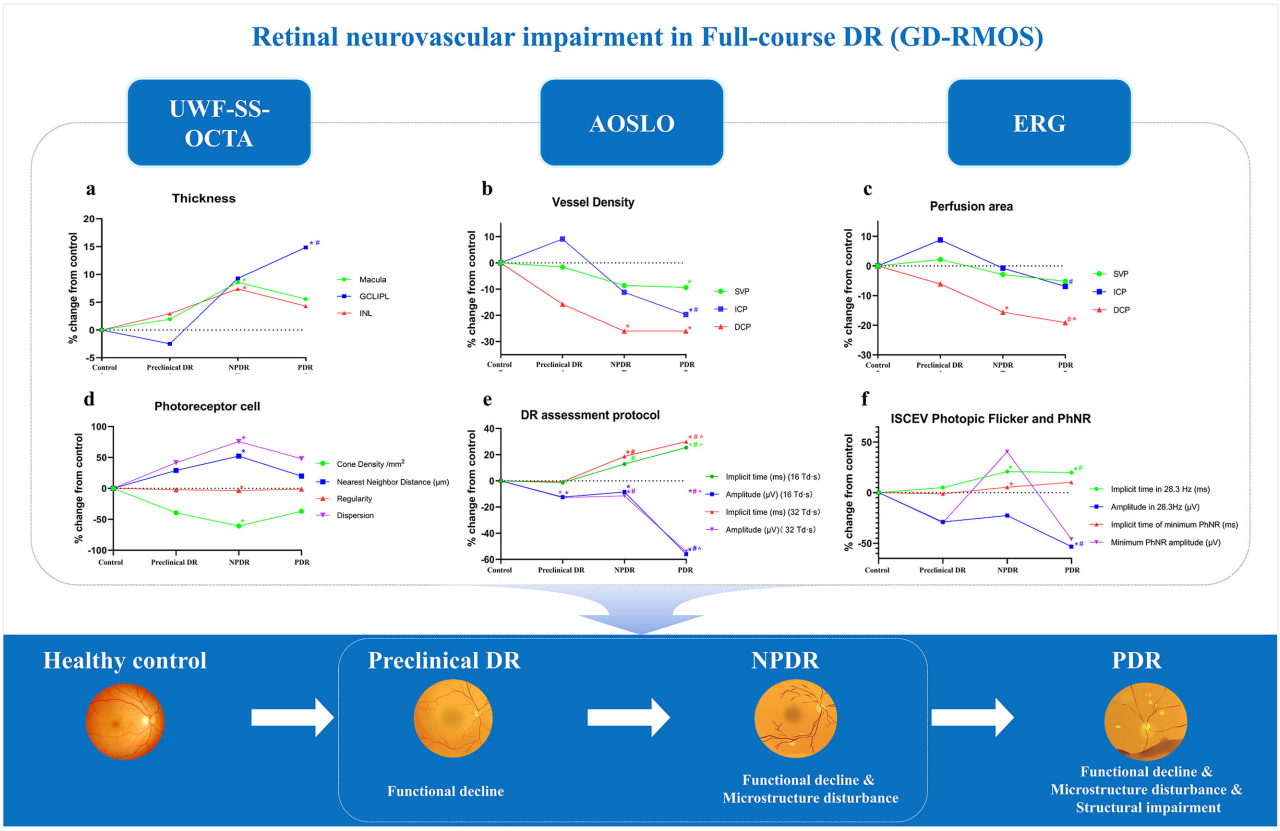

Figure 1. Graphical abstract. The UWF-SS-OCTA means ultra-widefield swept-source optical coherence tomography angiography. The AOSLO means adaptive optics scanning light ophthalmoscopy. The ERG means electroretinography. ISCEV means International Society for Clinical Electrophysiology of Vision. The preclinical DR means patients with diabetes without clinically detectable retinopathy. The NPDR means nonproliferative diabetic retinopathy. The PDR means proliferative diabetic retinopathy. GCL + IPL means ganglion cell layer and internal plexiform layer. INL means inner nuclear layer. VD means vessel density. PA means perfusion area. SVP means superficial vascular plexus. ICP means intermediate capillary plexus. DCP means deep capillary plexus. PhNR means photopic negative response. ANOVA adjusted the LSD test or Tamhane's T2 test with age, duration of diabetes, and HbA1c (*P < 0.05 vs. the control group; #P < 0.05 vs. the no DR group; and ^P < 0.05 vs. the NPDR group).

significantly in NPDR compared with the control group (both $P < 0.05$). The thickness of the GCL + IPL increased significantly only in PDR compared with the control group ($P = 0.036$). The VD of SVP showed a gradual decline in full-course DR, but there was a significant change in PDR ($P = 0.046$) compared with the control group. The VD of ICP showed a decreasing trend in the full-course DR, although it was not significant compared with the control group. The VD of DCP showed a slow decrease with the progression of the disease, and compared with the control group, there

Table 1. Baseline Demographic Characteristics of the Preclinical DR, the NPDR, the PDR, and the Healthy Group

	Overall (n = 81)	Healthy (n = 23)	Preclinical DR (n = 23)	NPDR (n = 13)	PDR (n = 22)	P Value
Age, mean (SD)	67.69 (9.74)	71.52 (9.02)	70.41 (9.13)	67.00 (5.12)	61.91 (10.18)	**0.004**
Gender, n (%)						0.589
Female	40 (49.38)	11 (47.83)	14 (60.87)	6 (46.15)	9 (40.91)	
Male	41 (50.62)	12 (52.17)	9 (39.13)	7 (53.85)	13 (59.09)	
Smoker, n (%)						0.588
No	59 (92.19)	16 (94.12)	17 (94.44)	9 (100.00)	17 (85.00)	
Yes	5 (7.81)	1 (5.88)	1 (5.56)	0 (0.00)	3 (15.00)	
Drinker, n (%)						0.146
No	59 (92.19)	17 (100.00)	17 (94.44)	9 (100.00)	16 (80.00)	
Yes	5 (7.81)	0 (0.00)	1 (5.56)	0 (0.00)	4 (20.00)	
Duration of diabetes, mean (SD)	8.73 (8.80)	0.00 (0.00)	7.43 (6.50)	6.00 (NA)	14.57 (8.26)	**<0.001**
HbA1c, n (%)	6.76 (1.45)	5.85 (0.66)	6.61 (0.46)	8.33 (2.63)	7.10 (1.23)	**<0.001**
eGFR, mean (SD)	64.29 (25.15)	64.88 (27.97)	46.52 (7.55)	72.07 (35.91)	87.01 (3.34)	0.291
Cholesterol, mean (SD)	4.82 (1.40)	4.96 (1.12)	4.65 (1.80)	5.33 (1.49)	4.60 (1.34)	0.635

DR, diabetic retinopathy; eGFR, glomerular filtration rate; HbA1c, glycated hemoglobin; NA,not applicable; NPDR, nonproliferative diabetic retinopathy; PDR, proliferative diabetic retinopathy.

Statistical significance was set at $P < 0.05$ and tested using-way ANOVA. Bold values indicate statistically significant results.

Table 2. Comparison of DR Assessment Protocol Results for the Preclinical DR, the NPDR, the PDR, and the Healthy Group

Parameters	Mean (SD) Healthy ($n = 23$)	Preclinical DR ($n = 23$)	NPDR ($n = 13$)	PDR ($n = 22$)	*P* Value (Healthy vs. Preclinical DR)	P Value (Healthy vs. NPDR)	P Value (Healthy vs. PDR)
Implicit time, ms (16 Td·s)	30.58 (1.50)	30.16 (2.32)	34.51 (4.48)	38.37 (4.87)	0.999	0.208	**<0.001**
Amplitude, μV (16 Td·s)	16.61 (7.41)	14.56 (6.67)	15.20 (6.60)	7.31 (3.09)	**0.003**	**0.020**	**<0.001**
Implicit time, ms (32 Td·s)	29.32 (1.51)	29.14 (1.87)	34.81 (5.12)	38.14 (6.06)	0.690	**0.004**	**<0.001**
Amplitude, μV (32 Td·s)	20.37 (8.30)	17.77 (9.06)	18.04 (8.20)	9.35 (3.90)	**0.018**	**0.042**	**<0.001**

DR, diabetic retinopathy; NPDR, nonproliferative diabetic retinopathy; PDR, proliferative diabetic retinopathy.

ANOVA adjusted the LSD test or Tamhane's T2 test with age, duration of diabetes, and HbA1c. Bold values indicate statistically significant results.

Table 3. Comparison of UWF-SS-OCTA Results for the Preclinical DR, the NPDR, the PDR, and the Healthy Group, Respectively

Parameters	Mean (SD) Healthy ($n = 23$)	Preclinical DR ($n = 23$)	NPDR ($n = 13$)	PDR ($n = 22$)	P Value (Healthy vs. Preclinical DR)	P Value (Healthy vs. NPDR)	P Value (Healthy vs. PDR)
Thickness							
Macula	207.44 (18.50)	211.49 (9.72)	225.23 (30.06)	219.01 (29.94)	0.546	**0.026**	0.090
GCL + IPL	29.50 (5.28)	28.77 (3.71)	32.24 (6.82)	33.89 (10.15)	0.718	0.254	**0.036**
INL	29.73 (2.64)	30.61 (1.00)	31.93 (2.54)	31.01 (4.49)	0.316	**0.036**	0.152
Vessel density							
SVP	21.51 (3.61)	21.17 (3.08)	19.66 (4.45)	19.50 (2.37)	0.729	0.113	**0.046**
ICP	12.67 (3.43)	13.82 (5.13)	11.25 (5.79)	10.18 (2.88)	0.364	0.343	0.055
DCP	6.85 (2.95)	5.77 (2.05)	5.07 (1.79)	4.82 (2.50)	0.137	**0.038**	**0.006**
Perfusion area							
SVP	56.10 (10.31)	57.33 (10.92)	54.50 (3.05)	53.21 (6.53)	0.636	0.602	0.274
ICP	41.12 (7.57)	44.74 (13.61)	40.82 (4.84)	38.29 (3.95)	0.166	0.921	0.283
DCP	39.46 (7.77)	37.07 (12.16)	33.31 (7.06)	31.92 (4.40)	0.343	**0.041**	**0.004**

DCP, deep capillary plexus; DR, diabetic retinopathy; GCL + IPL, ganglion cell layer and internal plexiform layer; gPDR, proliferative diabetic retinopathy; ICP, intermediate capillary plexus; INL, inner nuclear layer; NPDR, nonproliferative diabetic retinopathy; SVP, superficial vascular plexus.

ANOVA adjusted the LSD test or Tamhane's T2 test with age, duration of diabetes, and HbA1c. Bold values indicate statistically significant results.

was a significant difference in the NPDR ($P = 0.038$) and PDR ($P = 0.006$). The PA of SVP and ICP showed a slight decrease insignificantly. The PA of DCP decreased significantly in NPDR ($P = 0.041$) and PDR ($P = 0.004$) compared with the control group.

The Transformation of Photoreceptor Cell Parameters Throughout DR

The photoreceptor cell relative results among the subgroups were demonstrated in Supplementary Table S3. The density cones, nearest neighbor distance, regularity, and dispersion were found to be significant in NPDR compared with the control group (all $P < 0.05$) after adjustment for age, duration of diabetes, and HbA1c. There was no significant difference among other groups in photoreceptor cell relative results compared with the control group (all $P > 0.05$).

Correlation Analysis Between the Ocular Structural and Functional Parameters

Correlation analysis between the ocular structural and functional parameters are shown in Figure 2 and Supplementary Table S4. Delayed implicit time for 16 Td·s was associated with the thickness of GCL + IPL ($r = 0.563$, $P = 0.025$). Delayed implicit time for 32 Td·s was positively associated with the density cones ($r = -0.782$, $P = 0.043$), the thickness of the macula ($r = 0.567$, $P = 0.024$), the thickness of GCL + IPL ($r = 0.667$, $P = 0.006$), the VD of SVP ($r = -0.649$, $P = 0.008$), the VD of ICP ($r = -0.609$, $P = 0.014$), and the PA of DCP ($r = -0.519$, $P = 0.041$). Delayed implicit time for PhNR was associated with regularity ($r = -0.812$, $P = 0.033$) and the VD of ICP ($r = -0.509$, $P = 0.046$). The decreased amplitude for PhNR was associated with density cones, NND, and dispersion ($r = -0.946$, $P = 0.005$; $r = 0.913$, $P = 0.012$; and $r = 0.782$, $P = 0.043$, respectively). The decreased amplitude for PhNR was also associated with the thickness of GCL + IPL ($r = 0.568$, $P = 0.023$), and the VD of SVP and ICP ($r = -0.635$, $P = 0.010$; and $r = -0.604$, $P = 0.015$, respectively). The delayed implicit time for ISCEV Photopic Flicker was positively associated with the thickness of macula, GCL + IPL, and INL ($r = 0.656$, $P = 0.007$; $r = 0.704$, $P = 0.003$; and $r = 0.583$, $P = 0.019$, respectively), and the VD of SVP, ICP, and DCP ($r = -0.624$, $P = 0.011$; $r = -0.625$, $P = 0.011$; and $r = -0.526$, $P = 0.038$, respectively). The decreased amplitude for ISCEV Photopic Flicker was positively associated with the thickness of the GCL + IPL ($r = -0.562$, $P = 0.025$, respectively; see Supplementary Table S4).

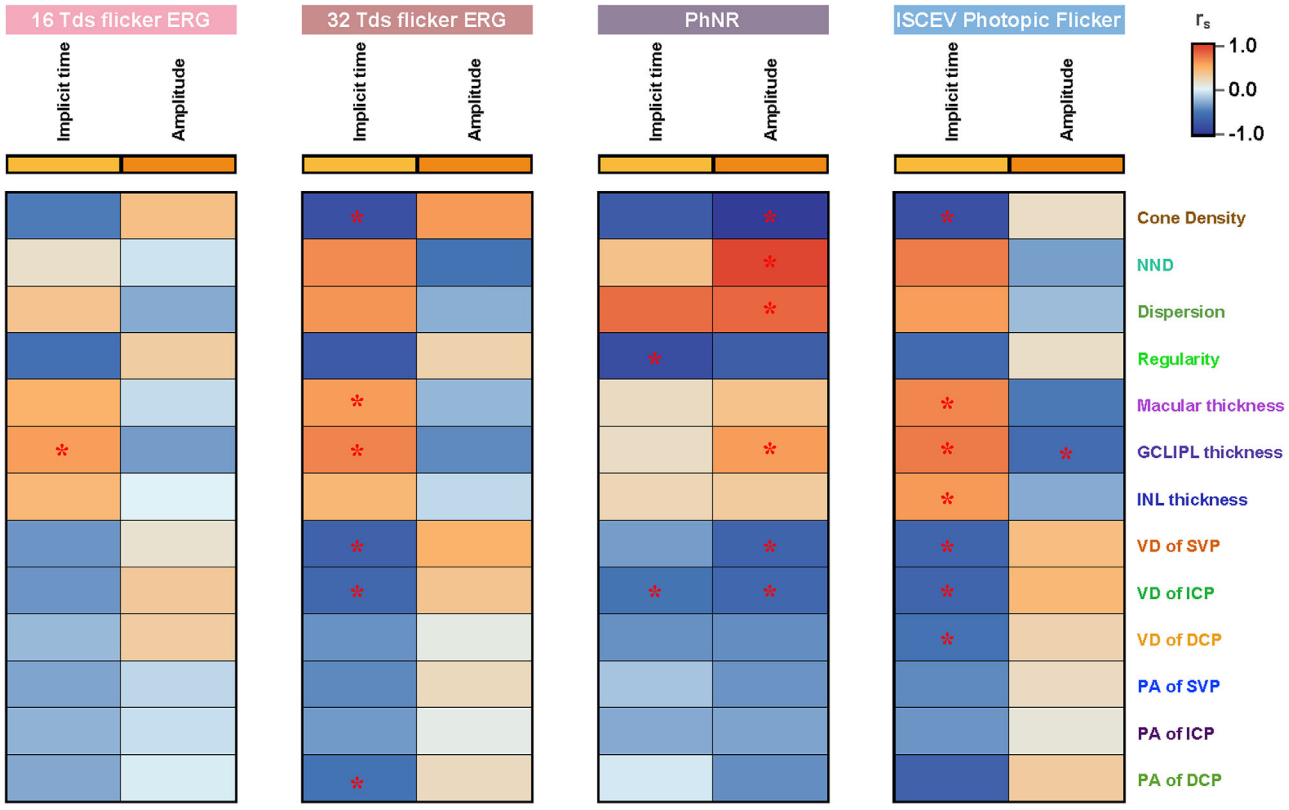

Figure 2. Correlation between ERG parameters and structural parameters. GCL + IPL means ganglion cell layer and internal plexiform layer. INL means inner nuclear layer. VD means vessel density. PA means perfusion area. SVP means superficial vascular plexus. ICP means intermediate capillary plexus. DCP means deep capillary plexus. ISCEV means International Society for Clinical Electrophysiology of Vision. PhNR means photopic negative response. Spearman Correlation analyses were used and adjusted with age, duration of diabetes, and HbA1c (*$P < 0.05$).

Discussion

In the current study, we evaluated the impact of DR on the neurovascular structure and function by applying the ERG, UWF-SS-OCTA, and AOSLO simultaneously. Our data showed that with the progression of DR, functional impairment occurred earliest in the preclinical DR, followed by visual cell impairment, a decrease of VD and PA in SVP, ICP, and DCP, and changes in thickness. Impairments in vascular, neural, and cellular structures were significantly associated with the decreased cone pathway function.

The results of flicker ERG in our study suggested that as the DR progresses, patients with DR experience a decline in overall cone pathway function, including the bipolar cell layer and the GCL. ERG parameters are considered sensitive markers of early neuronal abnormalities.[24,25] The cone pathway function relies on the integrity of both neural and vascular structures. In our study, although there was no statistical difference between patients with preclinical DR and the control group in retinal structure, including optic cells, thickness, and perfusion, there was a tendency for damage. ERG has shown signs of significant impairment of cone pathway function during the preclinical DR period, which is consistent with previous studies.[8,26] At the same time, our results showed that the bipolar cell layer function was impaired in NPDR and the ganglion cell function was impaired in PDR, which may be attributed to attenuated feedback occurring early in the retina at the synapse of cone photoreceptors and OFF bipolar cells in patients with NPDR and progressive loss of GCIPL in DR progression.[27,28]

The UWF-SS-OCTA improves the ability to identify peripheral DR lesions compared with standard imaging. More and more evidence has addressed that patients with diabetes have varying degrees of neurovascular damage as the disease progresses.[29–31] Eyes with any DR had thicker macular, and such thickening was most prominent in those with moderate or worse DR.[29] In addition, the study showed that the thickness of GCL + IPL and INL were increased in NPDR compared with controls.[31] However, in our cohort, there was a tendency for macular, GCL + IPL, and INL thickening in both preclinical DR and NPDR, whereas there was a decrease in the macular and INL thickness in PDR, which may be related to the severity of DR. Previous studies found that there were considerable differences in retinal layer structuring based on the severity of DR.[30] The inner retina has higher metabolic demands and relatively lower perfusion, which makes it more vulnerable to the metabolic stress induced by diabetes.[32] Therefore, more evidence is needed to clarify the changes in neurovascular structures. Similarly, the reduction of VD and PA in patients with DR has been found in previous studies.[4,33] Altered VD and PA may be due to the disruption of retinal neurovascular autoregulation, which could dynamically regulate blood flow in response to metabolic demands.[34] Besides, endothelial cell injury is a central pathogenic response to chronic hyperglycemia and initiates the progressive ischemic characteristic of DR.[35] The retinal capillary becomes acellular once

the dropout of endothelial cells begins, which may lead to reduced VD and PA in the retina.[35] Our results align with previous studies demonstrating that UWF-SS-OCTA had high sensitivity and specificity in detecting VD and PA, crucial for evaluating DR progression and treatment courses.[36,37]

This study has assessed the relationship between photoreceptor cell morphology and different stages of the full-course DR using the AOSLO system. In our study, we found significantly decreased cone density, decreased regularity, increased NND, and increased dispersion in the NPDR group compared with healthy controls after adjusting for age, duration of diabetes, and HbA1c, consistent with previous research.[15] Diabetic retinal abnormalities seen in early to moderate NPDR include pericyte loss and basement membrane thickening, which are potentially difficult to detect by clinical examination.[15] Previous studies showed that the AOSLO system allows observation of cellular structures in living human eyes and reveals retinal microstructures, such as the nerve fiber layer, photoreceptors, RPE cells, and retinal vasculature.[38] Interestingly, cone density and cone spacing have been reported in cross-sectional studies of patients with retinal degeneration to provide more sensitive measures of disease severity than visible changes on optical coherence tomography (OCT) or decline in visual acuity.[39–42] Decreased regularity of cone arrangement is consistently associated with the presence of diabetics and increasing DR severity.[14] Thus, abnormality of cone density, regularity, NND, and dispersion in different disease courses may reflect the severity of DR progression, and our results may reveal the relationship between full-course DR and deterioration of neuronal metabolism and phototransduction alteration.

In addition, thickness changes, blood perfusion, and cell microstructure were related to functional changes in this study. There was an overall tendency for retina, GCL + IPL, and INL thickening in patients with DR, which may be the cause of functional impairment.[8,29,31] The flicker response under 28.3 Hz light stimuli is produced by the ON and OFF pathway activity, and postreceptoral ON and OFF components contribute substantially to the sine-wave flicker ERG at higher stimulus frequencies.[43] The VD and PA detected by optical coherence tomography angiography (OCTA) perfectly reveal the perfusion of postreceptoral ON and OFF components, which indicates that the decrease in perfusion is closely related to the decline of function.[8,43] Furthermore, photoreceptor cells are part of the cone pathway, and the damage to the cone pathway was visualized by ultra-microscopic fundus imaging.[14,44] Taken together, we presumed that the functional changes in patients with DR might result from neurovascular impairment, and ERG may serve as a sensitive marker to predict the progression of DR.

There are several limitations in the study. First, the sample size of the research was relatively small, and more patients with NPDR are still needed to enhance the study's validity and the generalizability of its conclusions. However, after our sample size calculation in the Methods section, the sample size of this study is scientifically feasible. Second, this study was based on the international clinical diabetic retinopathy grouping. We plan to perform a more detailed grouping of DR and conduct associated proteomic mechanism analysis. Third, this is a cross-sectional study, so no conclusions can be drawn about causality. Therefore, further studies are needed to investigate the longitudinal development of neural function and structural impairments. Finally, we only focused on the functional changes in the cone pathway of the retina and ignored the rod pathway. To fully assess the function of the retina, a comprehensive understanding of the rod pathways is essential.

In conclusion, we found that functional impairments might precede the presence of visible retinal lesions in preclinical DR. This has positioned ultra-wide angle or more microscopic instruments for use in clinical scenarios, primarily as exploratory outcome measures or biomarkers for early screening of DR or monitoring DR progression and treatment response.

Acknowledgments

The authors thank all the members of the Guangdong Diabetic Retinopathy Multiple-omics Study (GD-RMOS) group for helping with patient recruitment and the Robotrak Technologies Co., Ltd for equipment support.

Supported by the National Natural Science Foundation of China (82171075, 82301260, 82271125, 82301205), China Postdoctoral Science Foundation (2024T170185), the Science and Technology Program of Guangzhou, China (20220610092), the launch fund of Guangdong Provincial People's Hospital for NSFC (8217040546, 8220040257, 8217040449, 8227040339), Guangdong Basic and Applied Basic Research Foundation (2023B1515120028), the Medical Scientific Research Foundation of Guangdong Province (A2021378), Brolucizumab Efficacy and Safety Single-Arm Descriptive Trial in Patients with Persistent Diabetic Macular Edema (BEST) (2024-29). The funders had no role in the study design, data collection, data analysis, data interpretation, or report writing.

Author Contributions: C. Lai and T. Su: conception and design. C. Lai, T. Su, J. Cao, Q. Li, Z. Du, Y. Wang, S. Wang, Q. Wu, Y. Hu, Y. Fang, H. Liao, Z. Zhu, and X. Shang: data collection, analysis and/or interpretation. C. Lai and T. Su: drafting the article. X. Zhang, M. He and H. Yu: final approval of the version to be published. All authors revised the article critically for important intellectual content. All authors read and approved the final manuscript.

Disclosure: **C. Lai**, None; **T. Su**, None; **J. Cao**, None; **Q. Li**, None; **Z. Du**, None; **Y. Wang**, None; **S. Wang**, None; **Q. Wu**, None; **Y. Hu**, None; **Y. Fang**, None; **H. Liao**, None; **Z. Zhu**, None; **X. Shang**, None; **M. He**, None; **H. Yu**, None; **X. Zhang**, None

References

1. Flaxel CJ, Adelman RA, Bailey ST, et al. Diabetic retinopathy preferred practice pattern. *Ophthalmology*. 2020;127(1):P66–P145.
2. Ji L, Tian H, Webster KA, Li W. Neurovascular regulation in diabetic retinopathy and emerging therapies. *Cell Mol Life Sci*. 2021;78(16):5977–5985.
3. Srinivasan S, Sobha S, Rajalakshmi R, et al. Retinal structure-function correlation in type 2 diabetes. *Eye (Lond)*. 2022;36(10):1865–1871.
4. Cao D, Yang D, Huang Z, et al. Optical coherence tomography angiography discerns preclinical diabetic retinopathy in eyes of patients with type 2 diabetes without clinical diabetic retinopathy. *Acta Diabetol*. 2018;55(5):469–477.
5. Kurata K, Hosono K, Hotta Y. Long-term clinical course of 2 Japanese patients with PRPF31-related retinitis pigmentosa. *Jpn J Ophthalmol*. 2018;62(2):186–193.
6. Lindsay R, Krege JH, Marin F, Jin L, Stepan JJ. Teriparatide for osteoporosis: importance of the full course. *Osteoporos Int*. 2016;27(8):2395–2410.

7. Salvi L, Plateroti P, Balducci S, et al. Abnormalities of retinal ganglion cell complex at optical coherence tomography in patients with type 2 diabetes: a sign of diabetic polyneuropathy, not retinopathy. *J Diabetes Complications*. 2016;30(3):469–476.
8. Zeng Y, Cao D, Yu H, et al. Early retinal neurovascular impairment in patients with diabetes without clinically detectable retinopathy. *Br J Ophthalmol*. 2019;103(12):1747–1752.
9. Vujosevic S, Midena E. Retinal layers changes in human preclinical and early clinical diabetic retinopathy support early retinal neuronal and Müller cells alterations. *J Diabetes Res*. 2013;2013:905058.
10. Ashraf M, Sampani K, Clermont A, et al. Vascular density of deep, intermediate and superficial vascular plexuses are differentially affected by diabetic retinopathy severity. *Invest Ophthalmol Vis Sci*. 2020;61(10):53.
11. Luu CD, Szental JA, Lee SY, Lavanya R, Wong TY. Correlation between retinal oscillatory potentials and retinal vascular caliber in type 2 diabetes. *Invest Ophthalmol Vis Sci*. 2010;51(1):482–486.
12. Wu H, Zhang G, Shen M, et al. Assessment of choroidal vascularity and choriocapillaris blood perfusion in anisomyopic adults by SS-OCT/OCTA. *Invest Ophthalmol Vis Sci*. 2021;62(1):8.
13. Lammer J, Karst SG, Lin MM, et al. Association of microaneurysms on adaptive optics scanning laser ophthalmoscopy with surrounding neuroretinal pathology and visual function in diabetes. *Invest Ophthalmol Vis Sci*. 2018;59(13):5633–5640.
14. Lammer J, Prager SG, Cheney MC, et al. Cone photoreceptor irregularity on adaptive optics scanning laser ophthalmoscopy correlates with severity of diabetic retinopathy and macular edema. *Invest Ophthalmol Vis Sci*. 2016;57(15):6624–6632.
15. Burns SA, Elsner AE, Chui TY, et al. In vivo adaptive optics microvascular imaging in diabetic patients without clinically severe diabetic retinopathy. *Biomed Opt Express*. 2014;5(3):961–974.
16. Diagnosis and classification of diabetes mellitus. *Diabetes Care*. 2014;37(Suppl 1):S81–S90.
17. Wilkinson CP, Ferris FL, 3rd, Klein RE, et al. Proposed international clinical diabetic retinopathy and diabetic macular edema disease severity scales. *Ophthalmology*. 2003;110(9):1677–1682.
18. Kato K, Kondo M, Sugimoto M, Ikesugi K, Matsubara H. Effect of pupil size on flicker ERGs recorded with RETeval System: new mydriasis-free full-field ERG system. *Invest Ophthalmol Vis Sci*. 2015;56(6):3684–3690.
19. Fukuo M, Kondo M, Hirose A, et al. Screening for diabetic retinopathy using new mydriasis-free, full-field flicker ERG recording device. *Sci Rep*. 2016;6:36591.
20. Tanimoto N, Sothilingam V, Kondo M, Biel M, Humphries P, Seeliger MW. Electroretinographic assessment of rod- and cone-mediated bipolar cell pathways using flicker stimuli in mice. *Sci Rep*. 2015;5:10731.
21. Yamashita T, Kato K, Kondo M, et al. Photopic negative response recorded with RETeval system in eyes with optic nerve disorders. *Sci Rep*. 2022;12(1):9091.
22. Li K, Yin Q, Ren J, Song H, Zhang J. Automatic quantification of cone photoreceptors in adaptive optics scanning light ophthalmoscope images using multi-task learning. *Biomed Opt Express*. 2022;13(10):5187–5201.
23. Chung JO, Park SY, Lee SB, et al. Plasma galectin-3 concentration and estimated glomerular filtration rate in patients with type 2 diabetes with and without albuminuria. *Sci Rep*. 2022;12(1):16328.
24. Pescosolido N, Barbato A, Stefanucci A, Buomprisco G. Role of electrophysiology in the early diagnosis and follow-up of diabetic retinopathy. *J Diabetes Res*. 2015;2015:319692.
25. Tsay K, Safari S, Abu-Samra A, Kremers J, Tzekov R. Pre-stimulus bioelectrical activity in light-adapted ERG under blue versus white background. *Vis Neurosci*. 2023;40:E004.
26. Eggers ED, Carreon TA. The effects of early diabetes on inner retinal neurons. *Vis Neurosci*. 2020;37:E006.
27. McAnany JJ, Chen YF, Liu K, Park JC. Nonlinearities in the flicker electroretinogram: a tool for studying retinal dysfunction applied to early-stage diabetic retinopathy. *Vision Res*. 2019;161:1–11.
28. Kim K, Kim ES, Yu SY. Longitudinal relationship between retinal diabetic neurodegeneration and progression of diabetic retinopathy in patients with type 2 diabetes. *Am J Ophthalmol*. 2018;196:165–172.
29. Dai W, Tham YC, Cheung N, et al. Macular thickness profile and diabetic retinopathy: the Singapore Epidemiology of Eye Diseases Study. *Br J Ophthalmol*. 2018;102(8):1072–1076.
30. Mohammed S, Li T, Chen XD, et al. Density-based classification in diabetic retinopathy through thickness of retinal layers from optical coherence tomography. *Sci Rep*. 2020;10(1):15937.
31. Wanek J, Blair NP, Chau FY, Lim JI, Leiderman YI, Shahidi M. Alterations in retinal layer thickness and reflectance at different stages of diabetic retinopathy by en face optical coherence tomography. *Invest Ophthalmol Vis Sci*. 2016;57(9):Oct341–Oct347.
32. van Dijk HW, Kok PH, Garvin M, et al. Selective loss of inner retinal layer thickness in type 1 diabetic patients with minimal diabetic retinopathy. *Invest Ophthalmol Vis Sci*. 2009;50(7):3404–3409.
33. Hao J, Du J, Gu X, Zhang Y, Yang L, Zhang S. Changes in and the association of retinal blood perfusion and retinal nerves in diabetic patients without retinopathy. *Front Endocrinol (Lausanne)*. 2022;13:1036735.
34. Abcouwer SF, Gardner TW. Diabetic retinopathy: loss of neuroretinal adaptation to the diabetic metabolic environment. *Ann N Y Acad Sci*. 2014;1311:174–190.
35. Simó R, Stitt AW, Gardner TW. Neurodegeneration in diabetic retinopathy: does it really matter? *Diabetologia*. 2018;61(9):1902–1912.
36. Gong Y, Hu L, Wang L, Shao Y, Li X. WF SS-OCTA for detecting diabetic retinopathy and evaluating the effect of photocoagulation on posterior vitreous detachment. *Front Endocrinol (Lausanne)*. 2022;13:1029066.
37. Russell JF, Al-Khersan H, Shi Y, et al. Retinal nonperfusion in proliferative diabetic retinopathy before and after panretinal photocoagulation assessed by widefield OCT angiography. *Am J Ophthalmol*. 2020;213:177–185.
38. Lew YJ, Rinella N, Qin J, et al. High-resolution imaging in male germ cell-associated kinase (MAK)-related retinal degeneration. *Am J Ophthalmol*. 2018;185:32–42.
39. Zayit-Soudry S, Duncan JL, Syed R, Menghini M, Roorda AJ. Cone structure imaged with adaptive optics scanning laser ophthalmoscopy in eyes with nonneovascular age-related macular degeneration. *Invest Ophthalmol Vis Sci*. 2013;54(12):7498–7509.
40. Talcott KE, Ratnam K, Sundquist SM, et al. Longitudinal study of cone photoreceptors during retinal degeneration and in response to ciliary neurotrophic factor treatment. *Invest Ophthalmol Vis Sci*. 2011;52(5):2219–2226.
41. Ratnam K, Carroll J, Porco TC, Duncan JL, Roorda A. Relationship between foveal cone structure and clinical measures of visual function in patients with inherited retinal degenerations. *Invest Ophthalmol Vis Sci*. 2013;54(8):5836–5847.

Investigative Ophthalmology & Visual Science

42. Liu JH, Peter DO, Faldalen Guttormsen MS, et al. The mosaic of AII amacrine cell bodies in rat retina is indistinguishable from a random distribution. *Vis Neurosci*. 2022;39:E004.
43. Kondo M, Sieving PA. Primate photopic sine-wave flicker ERG: vector modeling analysis of component origins using glutamate analogs. *Invest Ophthalmol Vis Sci*. 2001;42(1):305–312.
44. Banerjee A, Pandurangan K, Joe A, Sachidanandam R, Sen P. Comparison of broadband and monochromatic photopic negative response in eyes of patients with diabetes with no diabetic retinopathy and different stages of diabetic retinopathy. *Indian J Ophthalmol*. 2021;69(11):3241–3248.

Investigative Ophthalmology & Visual Science